

Molecular findings and the plasmid-mediated resistance mechanism of *Staphylococcus aureus*

Kiran Fatima¹, Kashif Ali^{1*}, Khwaja Ali Hasan², Neha Farid¹, Mumtaz Hussain³, Kanwal Khan⁴, Khurshid Jalal⁵, Reaz Uddin⁴, Zahid Hussain³

¹ Department of Biosciences, Faculty of Life Sciences, Shaheed Zulfikar Ali Bhutto Institute of Science and Technology (SZABIST) University, Karachi, Pakistan.

² Molecular Biology & Structural Biochemistry Research Laboratory, Department of Biochemistry, University of Karachi, Karachi 75270, Pakistan.

³ Department of Chemistry, University of Karachi, Karachi, Pakistan.

⁴ Dr. Panjwani Center for Molecular Medicine and Drug Research, International Center for Chemical and Biological Sciences, University of Karachi, Karachi, Pakistan

⁵ HEJ Research Institute of Chemistry International Center for Chemical and Biological Sciences, University of Karachi, Karachi, Pakistan

* Corresponding Author:

Prof. Dr. Kashif Ali

Abstract- *Staphylococcus aureus* is well known for its pathogenicity contributed by the organism's ability to adapt to an intracellular existence. Ten *Staphylococci* isolates were obtained from soil, water, yogurt, and clinical samples. Biochemical assays were used to identify the isolates phenotypically, and then confirmed through 16S rRNA PCR. Moreover, resistance pattern to antibiotics were observed in *Staphylococcus aureus*. *In silico* studies were performed to understand the mechanistic properties for these triazole compounds against the identified RepA resistant protein. PCR results showed that the species identified were primarily as *Staphylococcus aureus*, *Staphylococcus sciuri*, *Staphylococcus xylous* and *Staphylococcus cohnii*. Moreover, the clinical isolate of *Staphylococcus aureus* was found to be resistant to methicillin and vancomycin. *S. aureus* have not harbored the *mecA*, *vanA*, and *aroE* genes, conferring resistance to these antimicrobials. Furthermore, 75% of the strains were not biofilm producers, however these isolates probed for the conserved replication initiator RepA gene, and the results indicated that the resistance to methicillin and vancomycin was plasmid-mediated. Synthesized compounds C1, C2, C3 and C4, showed antimicrobial activity against the strains. Molecular docking studies of these compounds against RepA showed the stable interactions, especially for C3. Therefore, it may be used as an effective antimicrobial against MRSA and VRSA. The present study revealed that resistance in the clinical strains of *S. aureus* is not encoded by *mecA* and *vanA* genes, however the association of plasmid-mediated RepA gene has been identified as the primary cause of the resistivity in these strains.

Keywords: Vancomycin Resistance *Staphylococcus aureus* (VRSA), Methicillin Resistance *Staphylococcus aureus* (MRSA), molecular mechanism, antimicrobial resistance

1. INTRODUCTION

Antimicrobial Resistance (AMR) is still a growing worldwide issue caused mostly by the widespread use of antimicrobials. It is a dynamic risk to health-related issues around the world with higher mortality and morbidity rate (Becker *et al.*, 2018). The growing problem of antibiotic resistance presents a significant challenge as the widespread use of antibiotics threatens a crucial medical breakthrough of the 20th century. Compared infections produced by susceptible strains; infections generated by resistant bacteria are associated with twice as many unfavorable consequences. These poor effects may be

clinical or economical and are primarily the result of antibiotic treatment failure or delay (Friedman *et al.*, 2016; Jalal *et al.*, 2021).

Methicillin-Resistant *Staphylococcus aureus* (MRSA), is a significant contributor to Healthcare-Associated Infections (HAIs) is getting more difficult to treat as it develops resistance to all available antibiotics (Enrigh *et al.*, 2002). Resistance to antibiotics is a widespread issue with *S. aureus*. Continual information has detailed the isolation of single- or multidrug-resistant pathogenic *S. aureus* (MRSA) strains from many sources, including nutrients, the atmosphere, and healthcare facilities (Deschaght *et al.*, 2009; Kallen *et al.*, 2010). In order to assess how presence of this microorganism can affect nutritional security and community health, it is crucial to distinguish between virulent and non-virulent strains.

The resistant gene *mecA* is shifted by SCC_{mec} (Staphylococcal cassette chromosome *mec*) as a moveable genetic material (Omran Navai *et al.*, 2017). Detection of *mecA* and *VanA* is important to identify the cause of resistance in *S. aureus* (Becker *et al.*, 2018). A plasmid harbors multidrug-resistance genes encoding additional resistance to many antibiotic mechanisms. Particularly, Plasmid harbor RepA resistance gene is responsible for antibiotic and foreign particles using catabolic pathway like degradation of hydrocarbons, utilization of lactose and certain antibiotic synthesis Plasmid curing is the way to control the cause of antimicrobial resistance in bacterial strains. To remove the plasmid from the bacteria, many chemical and physical methods are involved. For plasmid curing in *S. aureus*, different chemical agents such as Acridine Orange Base (AOB) and Ethidium Bromide (EtBr) are used. RepA gene helps in the regulating of virulence and resistance in *S. aureus* (Schumacher *et al.*, 2014). The replication initiator, RepA plasmid encoded protein is necessary for their transmission and propagation of resistance determinants. Therefore, these collective data could help to discover the molecular mechanisms through which a given replicon of RepA mediates resistance in *S. aureus* (Schumacher *et al.*, 2014). An important threat to human health results from MRSA's ability to spread this trait to other hazardous strains via the food supplies, DNA fragments, bacteria's genetic stock and Plasmids (Biswas *et al.*, 2015). Consequently, a replacement therapy against this bacterium is urgently needed to cure sickness without increasing the risk of resistance to new drugs.

By screening a library of altered triazoles, compounds were synthesized as a new lead triazoles drug with strong antibacterial action against clinically significant MRSA and VRSA isolates. Structural characterization of the underlying protein-ligand interaction is often necessary for the rational design of synthetic compounds therapies to discover new derivatives with a reduced toxicity profile against human (Rashdan and Shehadi, 2022).

The objective of current research was to investigate the resistance mechanisms of methicillin-resistant *S. aureus* (MRSA) and vancomycin-resistant *S. aureus* (VRSA) isolates from different sources to control the potential inhibitory effect of synthesized chemical against the RepA-resistant protein. The study also hoped to provide significant insights on the prevalence and features of *Staphylococcus aureus* in several samples, including clinical strains, soil, water, and yogurt.

2. MATERIALS AND METHODS

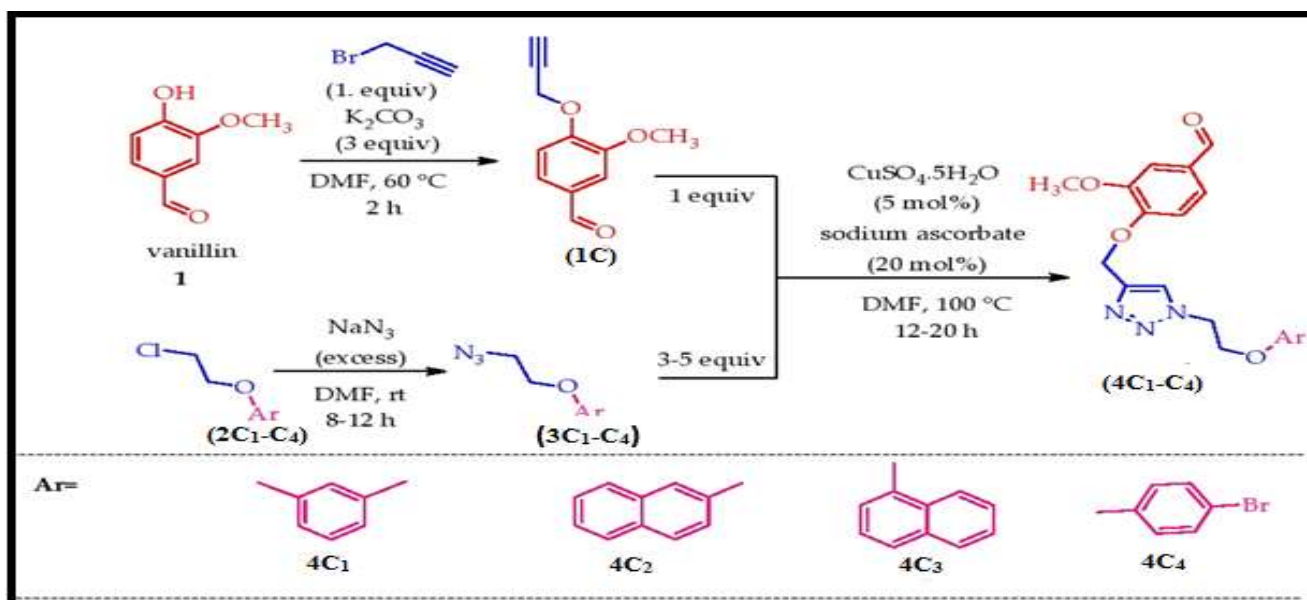
2.1. Characterization and Analytical Techniques Used

All reagents, chemicals and solvents used were analytical grade. Column chromatography using Silica gel 60 (0.043- 0.06 mm) Fluka was used for purification. Thin layer chromatography (TLC) was performed on Silica plates (60 F-254, Merck AG, Darmstadt, Germany). The ¹H-NMR information was collected with the help of a Bruker Avance 300 MHz instrument.

Chemical shifts (δ) in ppm and coupling constant (J) values in Hz were computed. EI-MS spectra were analyzed with a (JEOLJMS-600) mass spectrometer, while FT-IR spectra of substances were obtained using a VECTOR 22 spectrometer (BRUKER).

2.1.1 Standard operating procedure for compound synthesis (4C1-C4)

Following the procedure described by Zhang *et al.* (2005), alkyl azides (**3C1-C4**) were produced. This was accomplished by refluxing the compounds (**2C1-C4**) with sodium azide to produce the new compounds (**3C1-C4**) depicted in (Scheme 1). By reacting propargyl bromide with widely available 4-hydroxy-3-methoxybenzaldehyde (vanillin), potassium carbonate is utilized to create the alkyne molecule (**1C**) 3-methoxy-4-(prop-2-yn-1-yloxy) benzaldehyde (Scheme-1). Good yields of (**4C1-C4**) were obtained by treating the synthesized azides (**3C1-C4**) with compound (**1C**) 3-methoxy-4-(prop-2-yn-1-yloxy) benzaldehyde in the presence of Cu(I), a catalyst made locally by reducing $\text{CuSO}_4 \cdot 5\text{H}_2\text{O}$ with sodium ascorbate (Scheme 1). All of the synthesized triazoles (**4C1-C4**) had their structural properties evaluated by IR, NMR, mass spectrometry, and elemental analysis.



2.2 Isolation of Bacterial Strains

A total of 10 staphylococci cultures have been identified from local tap water, garden soil, food samples, and clinical samples. The strains were cultured on Mannitol Salt Agar (MSA), incubated at the temperature 37°C for time duration of 24 hours prior to observation (Zhang *et al.*, 2005)

2.3. Isolating and Phenotyping of *Staphylococcus aureus*

Staphylococcus aureus colonies grown on Mannitol Salt Agar (MSA) was further isolated by four streak method, and the plates were incubated at 37°C for 24 hours. Isolates were further identified via Gram staining, biochemical tests, morphological characterization along with detection of biofilm formation as described by Rodgers *et al.* (1999).

2.4. Biochemical Characterization of *Staphylococcus aureus*

The *S. aureus* strains were identified by biochemical tests such as the catalase test, coagulase test, growth on high salt concentration and mannitol fermentation, and hemolytic activity determination on sheep blood agar. The sheep blood agar was prepared by plating 15 ml of sheep blood with a concentration of 5% in Trypticase soy agar on 10 ml of blood agar (Morris *et al.*, 2001).

2.5. Molecular Identification

2.5.1. Genomic DNA Extraction

The genomic DNA of the bacteria was isolated by using the EZ-10 Spin Column Bacterial Genomic DNA Miniprep Kit (Bio Basic, Markham, Canada), with strict adherence to the outlined procedures. The purity and concentration of the isolated DNA were assessed using a NanoDrop spectrophotometer (ThermoFisher Scientific, Waltham, USA) (Zoetendal *et al.*, 2006).

2.5.2. Amplification of 16S rRNA Gene

Phenotypically identified strains of *S. aureus* were reconfirmed via 16S rRNA gene amplification using forward primer P1b16 'AGAGTTTGATCCTGGCTCAG' and reverse primer mlb16 'GGCTGCTGGCACGTAGTTAG' by initial denaturation at 95 °C for 3 min, followed by 35 cycles of template denaturation at 95 °C for 30 s, annealing at 55 °C for 30 s, an extension at 72 °C for 2 min, and the final extension at 72 °C for 5 min (Khan *et al.*, 2022). *S. aureus* ATCC 25923 and *S. aureus* ATCC 6538 was used as a positive control in this experiment. PCR products purification was performed by Biobase purification kit. Quantification of PCR product was done by NanoDrop spectrophotometer using optical density measurement. Sequencing for required PCR product was performed by Macrogen, South Korea (Thwala *et al.*, 2022).

2.6. Detection of Antimicrobial Resistances Genes

Resistance encoding genes in *S. aureus* were examined by using PCR amplification technique. Specific primers set for the *mecA* F (3'-AGAAGATGGTATGTGGAAGTTAG-5') and R (5'-ATGTATGTGCGATTGTATTGC-3'), and for *vanA* F (3'-GGCAAGTCAGGTGAAGATG-5') and R (5'-ATCAAGCGGTCAATCAGTTC-3'), were probed to amplify the targets. Housekeeping gene *aroE* (5'-ATCGGAAATCCTATTTACATTC-3') R (5'-GGTGTGTATTAATAACGATATC-3') and *Staphylococcus aureus* ATCC 29213 and *S. aureus* ATCC 6538 were used as a positive control for amplification as it had the two resistant genes of *mecA* and *vanA*. The *mecA* and *vanA* genes were amplified using a thermal cycler (Eppendorf, Germany) with a protocol consisting of an initial denaturation step at 95°C for 2 minutes, followed by 35 cycles of denaturation at 94°C for 1 minute, followed by 50°C for 50 seconds for annealing, and then 52°C for 40 seconds for elongation (Tamura *et al.*, 2011). Through the use of a 100bp DNA ladder and 1% agarose gel electrophoresis, the size and purity of the PCR products was evaluated.

2.7. Detection of biofilm formation by MtP assay

After incubating the *S. aureus* strains for 24 hours at 37°C on blood agar (BD Diagnostics), the Microtiter plate (MtP) test was carried out. The strains were grown overnight, and then diluted at a ratio of 1:200 in trypticase soy broth (TSB; Sigma-Aldrich) media. The media was supplemented with 0.25% glucose, and the end product was dispensed into a 96-well flat-bottom polystyrene microtiter plate. The plate was then incubated at a temperature of 37°C for a duration of 18 hours. After washing with phosphate-buffered saline (PBS) (pH 7.2), biofilm layer that had stuck to the plate was stained with crystal violet (ELI Tech Group Biomedical Systems), incubated for 1 min at room temperature, dried, and then solubilized in 1% w/v SDS. Using a spectrophotometer-ELISA reader, we measured the optical density at 490 nm (O.D₄₉₀) (Thermo Fisher Scientific). The test was repeated three times as described by Sofy *et al.* (2020). TSB was used as blank, whereas *S. aureus* ATCC 35984 as positive control, and *S. aureus* ATCC 12228 as negative control (Treves, 2010).

2.7.1. Detection of Biofilm Formation by CRA assay

Congo red agar test was used to analyze biofilm formation in a controlled environment. The CRA was prepared, inoculated, and monitored in accordance with Freeman *et al.* (1989) protocol. Bacterial colonies were obtained by growing culture on Congo red agar aerobically at 37°C for 24 hours. Colonies were found to be black in color for CRA-positive isolates and stayed red for CRA-negative ones.

2.8. Assessment of the Antimicrobial Efficacy and Determination of the Minimum Inhibitory Concentration (MIC)

Staphylococcus aureus strains were further identified as MRSA and VRSA by disk diffusion method. The antibiotics discs used were as followed: Sparfloxacin (30ug), Ciprofloxacin (5ug), Cephalexin (30ug), Clindamycin (2ug), Linezolid (30ug), Amikacin (30ug), Methicillin (5ug), Vancomycin (30ug), Compound Sulphamide (300ug), Streptomycin (10ug), Levofloxacin (30ug), Oxacillin (5ug), and Daptomycin (30ug). The strains were tested for antibiotic susceptibility in accordance with the standard reference guidelines (Patel *et al.*, 2015). Bacterial suspensions used were set at 0.5 McFarland Turbidity standard. Zone of inhibition was measured for each antibiotic after incubation at 37°C for 24 hours. To identify the MIC of the antibiotics which were ineffective against the strains, the E-test technique was used (Georgieva *et al.*, 2008).

2.9. Plasmid Curing and Intercalating Agents

Bacterial suspensions grown in Luria Bertani Broth (LB) were prepared as 0.5 McFarland Turbidity standard. In tubes containing 5ml of bacterial culture, 50µl of Acridine orange and Ethidium Bromide, each of 0.5mg/ml, were added separately, and incubated at 37°C for 24 hours (Liu *et al.*, 2012). After incubation, antibiogram assay was done as performed earlier (Leshem *et al.*, 2022).

2.10. Synthetization of Compounds

2.10.1 Experimental method for the synthesis of 1,4-disubstituted 1,2,3-triazoles (C1-C3)

Stirring a solution of 3-methoxy-4-(prop-2-yn-1-yloxy) benzaldehyde (1a) (1.0 g, 5.3 mmol) in 20 ml DMF, the corresponding 1-(3-azidoethoxy) aryl (2C₁-C₄) (10.6 mmol, 2 equiv) was added. As soon as the solution became clear, 20

mol% sodium ascorbate and 5 mol% copper (II) sulphate pentahydrate were added while stirring continuously. The reaction was maintained at 100°C for 16 hours monitored by TLC, solvent system; EtOAc: n-Hexane. The reaction mixture went from green to brown as it completed. DMF was extracted using filter paper and freeze drying. The reaction mixture was dissolved in dichloromethane, and then the solvent was evaporated at a low pressure. The products were purified through silica gel column chromatography, and the eluent utilized was a (4:6 v/v) ethyl acetate: n-hexane mixture.

2.10.2. Synthesis of Target Compound 4-((1-(2-(4-bromophenoxy) ethyl)-1H-1,2,3-triazol-4-yl) methoxy)-3-methoxybenzaldehyde (C1)

In accordance with standard procedures, 3-methoxy-4-(prop-2-yn-1-yloxy) benzaldehyde (**1C**) 100 mg (0.52 mmol) of 3-methoxy-4-(prop-2-yn-1-yloxy) benzaldehyde was dissolved in 10ml of DMF. Compound (**1C**) was reacted for 18 hours in a clear solution (1.0 g, 5.3 mmol) of CuSO₄·5H₂O and 20 mol% sodium ascorbate. Thin-layer chromatography using hexane and ethyl acetate (6:4 v/v) as a solvent was employed to monitor the reaction. Freeze drying was used to remove the DMF, then column chromatography was used to purify the compound. Light white solid was obtained with following characterization: Yield (81%); MP: 112-113 °C; R_f value: 0.65; IR (KBr, cm⁻¹): ν 3028 (=C-H, Ph), 1365 (C=N-*triazole*), 1025 (O-C, OCH₂), 1719 (C=O, CHO); ¹H NMR (300 HMz, CDCl₃): 8.30 (s, 1H-*triazole*), 5.20 (s, 1H, HN=C), 7.24 (d, 2H, Ar-H), 6.81 (d, 2H, Ar-H), 7.56 (d, 1H, Ar-H), 7.41 (d, 1H, Ar-H), 7.37 (s, 1H, Ar-H), 4.5 (t, 2H, Ar-CH₂CH₂), 3.80 (t, 2H, ArCH₂CH₂), 9.80 (s, 1H, Ar-CHO), 3.63 (s, 3H, Ar-CH₃); ESI-MS: *m/z* 430(M⁺ C₁₉H₁₈BrN₃O₄, calc. 432).

2.10.3. Synthesis of Target Compound 3-methoxy-4-((1-(2-(naphthalen-2-yloxy) ethyl)-1H-1,2,3-triazol-4-yl) methoxy) benzaldehyde (C2)

According to general procedure 3-methoxy-4-(prop-2-yn-1-yloxy) benzaldehyde (**1C**) 100 mg (0.52 mmol) of 3-methoxy-4-(prop-2-yn-1-yloxy) benzaldehyde was dissolved in 10 ml DMF. After clear solution formation (1.0 g, 5.3 mmol) 2-(2-azidoethoxy) naphthalene was reacted with compound (**1C**) in the presence of CuSO₄·5H₂O and sodium ascorbate 20 mol % for sixteen hours. The reaction progress was monitored with thin layer chromatography (TLC) by using Hexane and ethyl acetate (6:4 v/v) and DMF was evaporated through freeze drying and compound was purified with the help of column chromatography by using hexane and ethyl acetate. Light Brown gummy solid was obtained with following characterization: Yield (83%); MP: 122-123 °C; R_f value: 0.69; IR (KBr, cm⁻¹): ν 3025 (C=CHPh), 1305 (C=N-*triazole*), 1056 (O-CH₂), 1726 (C=O, CHO), ¹H NMR (300 MHz, DMSO-d₆): δ 9.51 (s, 1H, Ar-CHO), 8.22 (s, 1H-*triazole*), 5.20 (s, 1H, HN=C), 7.7 (s, 2H, Ar-H), 7.55 (d, 2H, Ar-H), 7.36 (d, 2H, Ar-H), 7.25 (d, 2H, Ar-H), 6.41 (s, 2H, Ar-H) 5.68 (s, 2H, ArOCH₂), 3.83 (t, 4H, OCH₂CH₂), 3.51 (s, 3H, ArOCH₃); ESI-MS: *m/z* 406 (M⁺, C₂₃H₂₁N₃O₄, calc. 403.43), *m/z* 239 (C₁₄H₁₃N₃O).

2.10.4. Synthesis of Target Compound 3-methoxy-4-((1-(2-(naphthalen-1-yloxy) ethyl)-1H-1,2,3-triazol-4-yl) methoxy) benzaldehyde (C3)

According to general procedure 3-methoxy-4-(prop-2-yn-1-yloxy) benzaldehyde (**1C**) 100 mg (0.52 mmol) of 3-methoxy-4-(prop-2-yn-1-yloxy) benzaldehyde was dissolved in 10 ml DMF. After clear solution formation (1.0 g, 5.3 mmol) 1-(2-azidoethoxy) naphthalene was reacted with compound 1a in the presence of CuSO₄·5H₂O and sodium ascorbate 20 mol% for 18 hrs. The reaction progress was monitored with thin layer chromatography (TLC) by using Hexane and ethyl acetate (6:4 v/v) and DMF was evaporated through freeze drying and compound was purified with the help of column

chromatography by using hexane and ethyl acetate. Light Brown gummy solid was obtained with following characterization; MP; 115-116 °C; Yield (85%); R_f value: 0.71; IR (KBr, cm^{-1}): ν 3025 (C=CHPh), 1305 (C=N-*triazole*), 1056 (O-CH₂), 1726 (C=O, CHO), ¹H NMR (300 MHz, CDCl₃): δ 8.22 (s, 1H-*triazole*), 5.68 (s, 1H, HN=C), 7.69 (s, 1H, Ar-H), 6.60 (s, 1H, Ar-H), 7.8 (s, 1H, Ar-H), 7.1 (s, 1H, Ar-H), 7.37 (d, 1H, Ar-H), 7.54 (d, 1H, Ar-H), 3.77 (t, 4H, ArCH₂CH₂), 9.51 (s, 1H, ArCHO), 3.51 (s, 3H, ArCH₃); ESI-MS: m/z 403 (C₂₃H₂₁N₃O₄, calc. 403).

2.10.5. General experimental method for the synthesis of 1,4-disubstituted 1,2,3-triazoles (C4)

In 100 ml round bottom flask stirrer a solution of 3-methoxy-4-(prop-2-yn-1-yloxy) benzaldehyde (**1C**) (1.0 g, 5.3 mmol) in 20 ml DMF, the corresponding 1,3-bis(2-azidoethoxy) benzene (10.6 mmol, 2 equiv) was added. As soon as the solution became clear, 20 mol% sodium ascorbate and 5 mol% copper (II) sulphate pentahydrate were added while stirring continuously. The reaction was maintained at 100 C for 16 hours (monitored by TLC, solvent system; EtOAc:n-Hexane). The reaction mixture went from green to brown as it completed. DMF was extracted using filter paper and freeze drying. The reaction mixture was dissolved in dichloromethane (DCM) and then the solvent was evaporated at a low pressure. The products were purified through silica gel column chromatography by using ethyl acetate:n-hexane mixture (4:6 v/v) as eluent.

2.10.6. Synthesis of Target Compound 4,4'-((1,1'-((1,3-phenylenebis(oxy)) bis(ethane-2,1-diyl)) bis(1H-1,2,3-triazole-4,1-diyl)) bis(methylene)) bis(oxy)) bis(3-methoxybenzaldehyde) (C4)

10ml DMF was used to dissolve 100 mg (0.52 mmol) of 3-methoxy-4-(prop-2-yn-1-yloxy) benzaldehyde (**1C**). 129 mg (1 mmol) of 1,3-bis(2-azidoethoxy) benzene was added after the creation of a clear solution, along with 5 mol% of copper sulphate pentahydrate and 20 mol% of sodium ascorbate. For 20 hours, the reaction was heated to reflux. The reaction's colour transitioned from green to brown. TLC analysis was used to keep track of the response. DMF was removed by filtering using filter paper and freeze drying. Filtration was done after dichloromethane was added to the reaction mixture. Hexane and ethyl acetate (6: 4 v/v) were used in silica gel column chromatography after the solvent had been evaporated. The obtained compound had the following properties: MP: 122-123 °C; Yield (80%); R_f value: 0.69; IR (KBr, cm^{-1}): ν 3025 (C=CHPh), 1305 (C=N-*triazole*), 1056 (O-CH₂), 1726 (C=O, CHO); ¹H NMR (300 MHz, DMSO-d₆): δ 9.51 (s, 1H, Ar-CHO), 8.22 (s, 1H, H-*triazole*), 7.7 (s, 2H, Ar-H), 7.55 (d, 2H, Ar-H), 7.36 (d, 2H, Ar-H), 7.25 (d, 2H, Ar-H), 6.41 (s, 2H, Ar-H) 5.68 (s, 2H, ArOCH₂), 3.83 (t, 4H, OCH₂CH₂), 3.51 (s, 3H, ArOCH₃);), ESI-MS: m/z 628 (C₃₂H₃₂N₆O₈, calc. 628).

2.11. In silico Analysis

Furthermore, *in silico* analysis was performed to gain comprehension of the molecular mechanism of the compound with the respective protein and interactions.

2.11.1. Retrieval and Preparation of Protein

A three-dimensional protein structure is the most crucial prerequisite for molecular docking. The 3D x-ray crystalline structure of protein showing possible inhibition from *in vitro* studies were searched for the structure in PDB databases. However, due to the unavailability of the protein structure, SWISSMODEL (Kiefer *et al.*, 2009) was used to model the 3D structure of protein for further investigation. Water, metal ions, cofactors, other molecules, and protein tetramer subunits

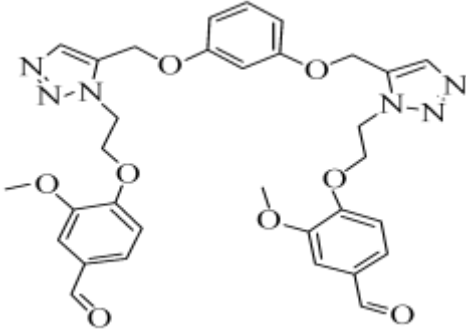
were all separated using the UCSF Chimera. Subsequent preparation of protein was accomplished using AutoDock v4.2 (Huey *et al.*, 2012). Development of the receptor requires the addition of all the hydrogen atoms, the incorporation of Kollman charges, and the fusing of non-polar hydrogen atoms (Morris *et al.*, 2001).

2.11.2. Compounds Retrieval and Preparation

The compounds were commercially synthesized having triazole as a parent compound i.e., C1, C2, C3 and C4 (Table 1). By utilizing the Open Babel programme (O'Boyle *et al.*, 2011), the collected 2D compound format was successfully converted into a 3D PDB file. As detailed in study by Jalal *et al.* 2021, the ligand's energy was reduced using the FROG2 programme (Miteva *et al.*, 2010), and the steepest descent technique with the MMFF94 force field over a period of 1500 steps. Subsequently, the compounds were ready for molecular docking investigations by using the AutoDock software. The optimized chemical library was saved in PDBQT format for future high-throughput screening, and gastieger charges were added, torsion was induced by rotating all rotatable bonds.

Table 1: Synthesized triazole composites details utilized in the current study as 1, 2, 3, and 4 with IUPAC names and structures.

S. No.	Compound ID	Compound Name	Compound Structure
1	C1	4-(2-(5-((4-bromophenoxy)methyl)-1H-1,2,3-triazol-1-yl)ethoxy)-3-methoxybenzaldehyde	
2	C2	3-methoxy-4-(2-(5-((naphthalen-1-yloxy)methyl)-1H-1,2,3-triazol-1-yl)ethoxy)benzaldehyde	
3	C3	3-methoxy-4-(2-(5-((naphthalen-2-yloxy)methyl)-1H-1,2,3-triazol-1-yl)ethoxy)benzaldehyde	

4	C4	4,4'-(((5,5'-((1,3-phenylenebis(oxy))bis(methylene))bis(1H-1,2,3-triazole-5,1-diyl))bis(ethane-2,1-diyl))bis(oxy))bis(3-methoxybenzaldehyde)	
---	----	--	--

2.11.3. Molecular Docking Studies

Molecular docking was used to examine the inhibitory effects and binding affinities of these compounds with the appropriate protein. A receptor protein and ligand were used in the docking analysis. In this study, we employed the Lamarckian Genetic Algorithm of ADT (AutoDock) to explore the active binding space. Previous research on the protein was consulted in order to locate the binding pocket. For docking purposes, a grid box was constructed around the receptor area, and the reported active residues were assigned corresponding labels. The grid center parameters were set at -8.444, -9.833, and -3.278, respectively with the grid center settings set to 66, 60, and 62 points on the X, Y, and Z-axis respectively. Using AutoDock v4.2 with 250 times Lamarckian GA settings, the maximum number of generations was 27,000, and the maximum number of assessments was 250,000 (Jalal *et al.*, 2021).

2.11.4. ADME Profiling and Toxicity Analysis

The compounds' physiochemical properties investigated to identify the most important variables that may affect their biological activity. Bioavailability, biopharmaceutical qualities, and drug similarity may be predicted by physicochemical analysis as well as the molecular weight of a compound and its permeability through skin, cells, and the digestive tract. Additionally, the drug's absorption, distribution, metabolism, and excretion (ADME) properties and other pharmacologically relevant characteristics were evaluated using the SwissADME program (Georgieva *et al.*, 2008). In addition, toxicity is a key obstacle while developing new drugs. We used the pkcsm program to calculate the acute toxicity of compounds in rats and mice, as well as their carcinogen pattern and acute toxicity.

2.12. Statistical Analysis

The SPSS (v.25) was used to analyze the data. The quantitative variables were subjected to a Mean and Standard Deviation analysis. We used Analysis of Variance (ANOVA) to compare the zone sizes. The statistically significance level used $p \leq 0.05$.

3. RESULT & DISCUSSION

3.1. Isolation and identification of Bacterial Strains

In this study, 10 samples were collected from water, garden soil, food and clinical wound and sepsis patient. Morphological studies using colony occurrence and gram staining confirmed that among them, only 4 strains were really *Staphylococcus aureus* after culturing the isolates on selective media i.e. Mannitol Salt Agar (MSA). When grown on MSA, pale yellow colonies indicated the growth of *Staphylococcus aureus* along with change in color of media from red to yellow. Gram staining showed purple-colored cocci shaped cells. The identified strains were named as KSA01, KSA02, KSA03, and KSA04. Morphological characterization of all the isolated strains has been summarized in Table 2.

Table 2: Showing the morphological characterization of all 10 isolated strains.

Characterization	Observations	KSA01	KSA02	KSA03	KSA04	Rest of remaining strains
Colony Characterization	Yellow colony formation	+	+	+	+	-
Gram Staining	Purple (gram +ve)	+	+	+	+	-

3.2 Biochemical Characterization of *Staphylococcus aureus* Strains.

The most important and basic phenotypic biochemical identifying markers of *Staphylococcus aureus* tests were catalase and coagulase. Results showed that all of the isolates tested positive for catalase and coagulase.

3.3. Molecular identification and phylogenetic clustering of *S. aureus*

The 16S rRNA and *aroE* gene amplicons confirmed the identification of 10 isolates of *S. aureus* recovered in this study followed by sequencing analysis of selected MDR strains. The nucleotide sequences of 16S rRNA gene obtained from MDR isolates have been deposited in GenBank under Accession No: KSA01 *Mammaliococcus sciuri* (MZ604307), KSA02 *Mammaliococcus sciuri* MZ604298, KSA03 *Staphylococcus aureus* strain ATCC 6538 (MZ686492), KSA04 *Staphylococcus aureus* MZ686493.

The phylogram in figure 1B revealed three distinct clades because of neighbor joining analysis of 16S ribosomal RNA (rRNA) sequences obtained from four MRSA isolates in this study and 11 sequences retrieved from the National Center for Biotechnology Information (NCBI) database on the basis of genetic similarity after comparison through the Basic Local Alignment Search Tool (BLAST). Fifteen 16S ribosomal DNA sequences were used to generate the phylogenetic tree using Molecular Evolutionary Genetic Analysis (MEGA-6) (Turnipseed, 2022). Consequently, it is infer that the identified strains showed close association with MRSA (Figure 1B).

3.4. Detection of Antibiotic Resistances and Housekeeping Genes in *S. aureus*

Multiplex PCR conferred the resistance genotypes in *S. aureus* strains, including *mecA*, *vanA*, and *aroE* of 310-750bp respectively (Figure 1A and Table 3) when compared with standard 1 kbp DNA ladder and the amplicons were separated through 1% agarose gel electrophoresis at 100V.

Primer		Direction of Sequences	Amplicon sizes (bp)	Ref.
<i>mecA</i>	F	GTAGAAATGACTGAACGTCCGATGA	310bp	29
	R	CCAATTCCACATTGTTTCGGTCTAA		
<i>vanA</i>	F	GGCAAGTCAGGTGAAGATG	713 bp	30
	R	ATCAAGCGGTCAATCAGTTC		
<i>aroE</i>	F	ATCGGAAATCCTATTTCACATTC	450 bp	31
	R	GGTGTGTATTAATAACGATATC		

Table 3: The 16S rRNA, *mecA*, *vanA*, and *aroE* primer sequences of *S. aureus*.

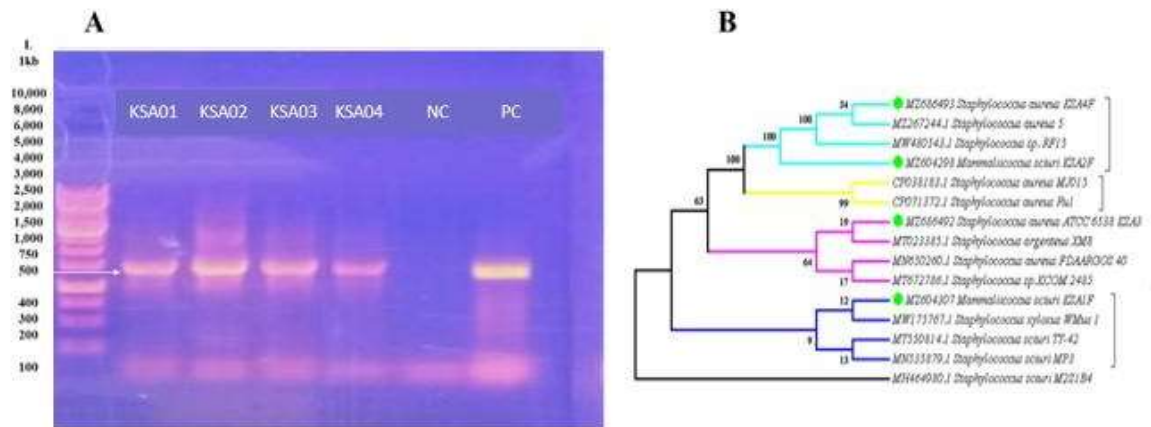


Figure 1: (A) Shows the genus specific 16 rRNA gene amplicons of *S. aureus* in. Lane 1: DNA marker (1 kb); Lanes 2(KSA01), Lanes 3(KSA02), Lanes 4(KSA03), and Lanes 5(KSA04), Lanes 6 Negative Control and Lanes 7 Positive Controls, (ATCC 33591). (B) Phylogenetic tree created using partial sequences of 16S rDNA of MRSA isolates and compared through 11 sequences exhibiting 99% phylogenetic association with other strains derived from BLAST findings. The clades distributed in phylogenetic tree confirmed the reliability and similarity between *Staphylococcus aureus* strains used in this study.

3.5. PCR Screening for Resistance & Housekeeping Genes:

The resistance *mecA* and *vanA* genes were not found in the isolates of *Staphylococcus aureus* by using PCR with a specific primer. The results obtained are highlighted in the Figure 2.

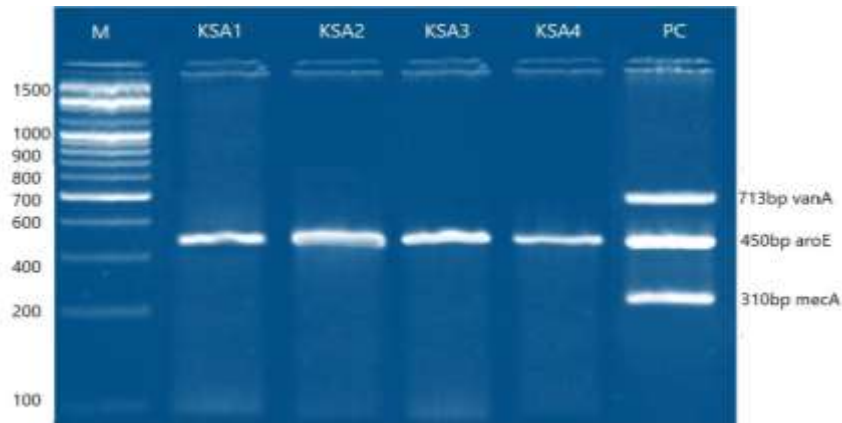


Figure 2: The PCR results of the *mecA*, *vanA* gene for *S. aureus* strains. Lane 1: DNA marker (100bp); Lanes 2, 3, 4 & 5 *S. aureus* samples; Lane 6: Positive control (ATCC 33591). No resistant Genes were found except housekeeping (*aroE*) gene.

3.6. Biofilms analysis

3.6.1. Detection of biofilm formation using the micro titre-plate (MtP) assay

According to the MtP assay, *S. aureus* strains exhibiting an O.D.490 reference value below 0.1 were classified as non-producers, while those with an O.D.490 value ranging from 0.1 to 1.0 were considered as weak biofilm producers. On the other hand, strains with an O.D.490 value above 1.0 were identified as strong biofilm producers (Table 4). Duplicate strains of each species were used in three separate biofilm formation assays (Treves, 2010).

Table 4: The tables represent the weak/no biofilm formed according to Ref. value as Weak<0.120, Moderate 0.120-0.199, High0.200-0.239, Strong high >0.240, Wavelength (OD490)

S. No.	Strain	Mean OD value	Biofilm formation	Ref. value	Ref. value
1	KSA 01	0.01	None/ Weak	<0.120	None/Weak
2	KSA 02	0.003	None/ Weak	0.120-0.199	Weak
3	KSA 03	0.00	None/ Weak	0.200-0.239	Moderate
4	KSA 04	0.00	None/ Weak	>0.240	High/Strong

Strains were assessed for biofilm generation using the MtP technique based on the intensity of their corresponding colour of absorbance, with strains with an O.D490 of 0.1 or below being labelled as non-producers (Figure 3a).

3.6.2 Detection of biofilm formation by CRA assay

The characterization of the isolates was based on the morphological appearance of the colony. Strong biofilm-producers were observed to form black colonies, while moderate biofilm producers formed blackish-red colonies. Weak or non-producers were observed to form pink colonies. Each strain was tested according to triplicate testing for biofilm production (Schumacher *et al.*, 2014) (Figure 3b).

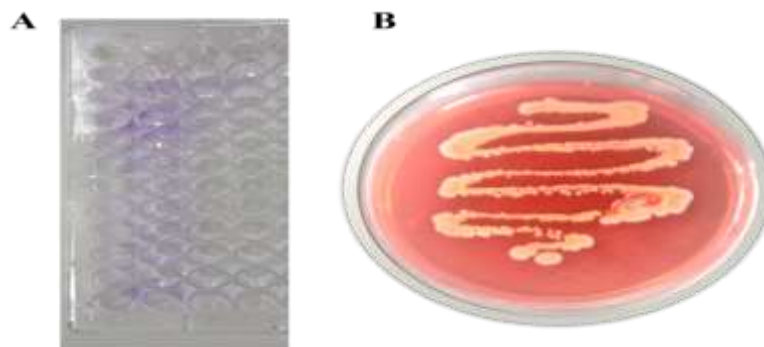


Figure 3: (A) biofilm detection via ELISA techniques showing the presence of biofilm (B) The identification of biofilms using Congo red dye. The screening of biofilm through the utilization of the Congo red agar method involved the identification of weak producers as pink colonies, while non-producers were identified as red smooth colonies.

3.7. Plasmid Curing in Bacteria with Intercalating Agents

Curing bacterial plasmid was done with the intercalating agents: Acridine Orange Base (AOB) and Ethidium Bromide (EtBr) with concentration of 0.5mg/ml. As seen in Figure 4, the control strains with plasmid expressed resistance to the antibiotics showed smaller zone of inhibition whereas the strains treated with AOB & EtBr were found to be sensitive towards the antibiotics. This is due to the removal of plasmid by treating with the curing agents. It led to the fact that the antibiotic resistance in the strains was contributed by the plasmid. It was also observed that EtBr has more potential as plasmid curing agent as compared to AOB.

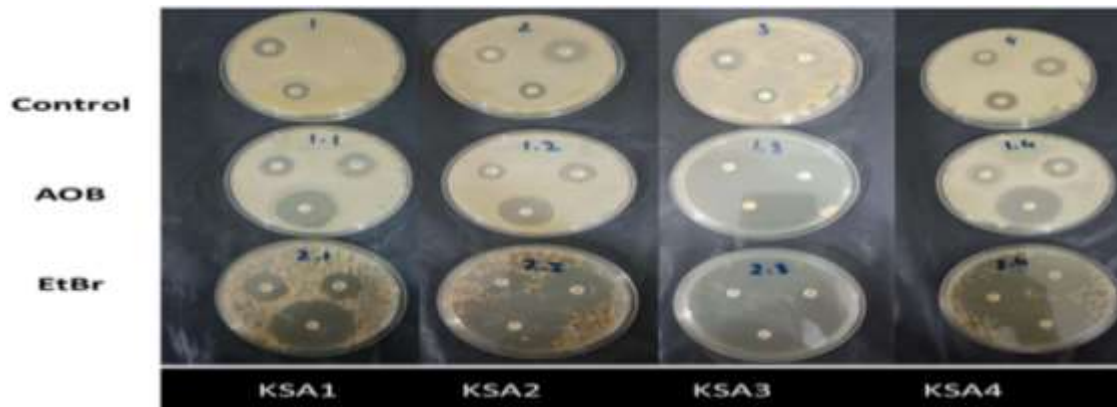


Figure 4: Control with plasmid and AOB & EtBr without plasmid. Control strains show resistivity while treated with curing agents show sensitivity against *S. aureus*.

3.8 Difference in Antibiotic Susceptibility Pattern before and After treatment of Curing agent

All of the *S. aureus* strains were found to be resistant to several antibiotics. The prevalence rate of MRSA was found to be more than 90% in this study. The resistance rate of antibiotics found 80% to 100%. Resistance of *Staphylococcus aureus* isolates to various antibiotics was found as: Sparfloxacin (80%), Ciprofloxacin (80%), Cephalexin (60%), Clindamycin (80%), Linezolid (80%), Amikacin (60%), Methicillin (100%), Vancomycin (95%), Compound Sulphamide (60%), Streptomycin (60%), Levofloxacin (60%), and Oxacillin (80%), Daptomycin (95%) as depicted in Figure 5a.

3.8.1. Antibiotic Susceptibility Pattern of Isolates After treatment of Intercalating Agents

The sensitivity rate of the strains towards antibiotics was found in the range of 60% – 80%. Sensitivity of *Staphylococcus aureus* isolates to various antibiotics: Sparfloxacin (60%), Ciprofloxacin (60%), Cephalexin (60%), Clindamycin (80%), Linezolid (80%), Amikacin (60%), Methicillin (100%), Vancomycin (95%), Compound Sulphamide (60%), Streptomycin (60%), Levofloxacin (60%), and Oxacillin (80%), Daptomycin (80%) as depicted in Figure 5b.

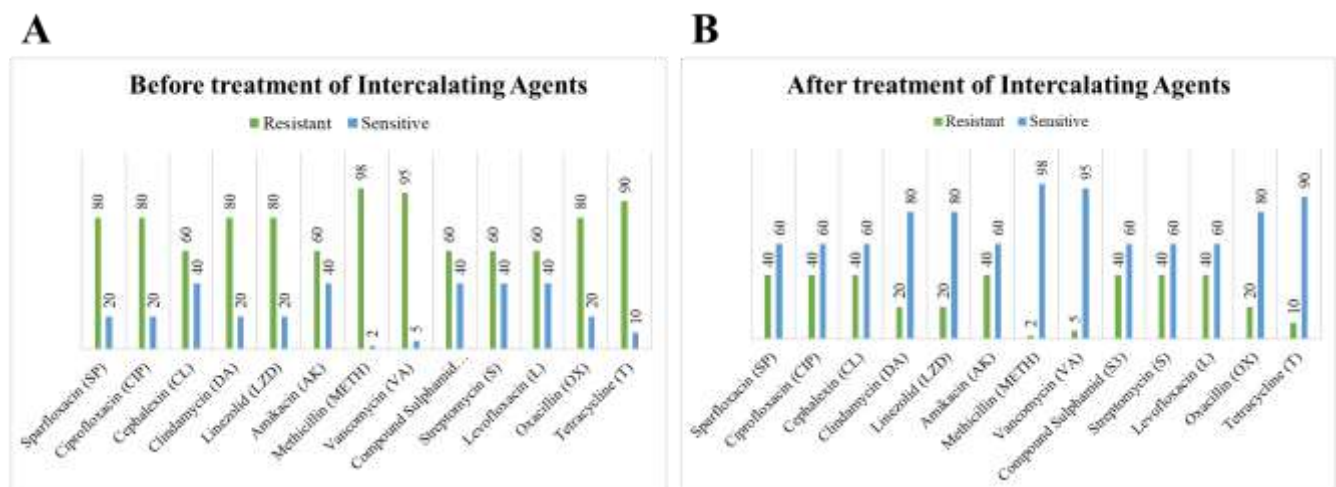


Figure 5: (A) Result of antibiotics susceptibility test on *S. aureus* isolates before plasmid treatment with intercalating agent
(B) Result of antibiotics susceptibility rate on *S. aureus* isolates after plasmid treatment with intercalating agent.

3.9. Antimicrobial Activity of Synthesized Compounds

Upon testing the triazole derivatives against the test strains namely KSA01, KSA02, KSA03, and KSA04, it was observed that the multi drug resistant strains were susceptible to the synthesized compounds. As shown in Figure 6, the MIC value for compound C3 was 100 $\mu\text{g/ml}$, which was effective concentration to inhibit *S. aureus* growth.



Figure 6: Antimicrobial activity of synthesized compounds showing the inhibition of *S. aureus* in different concentration. The compound 3d showing the most potential activity for the *S. aureus* inhibition.

3.10. In-silico Studies

3.10.1. Structure Modelling

It was analyzed through *in vitro* study that the resistivity pattern of *S. aureus* (MRSA) was primarily due to the presence of RepA (replication initiator protein A) gene within the plasmid. Therefore, the RepA sequence was retrieved from the plasmid (nucleotide sequence) and searched for the possible protein pattern. The blastx was performed to identify the possible proteins for the RepA gene. Consequently, RepA gene from the *Staphylococcus aureus* (ID: WP_172686042.1) showed a best hit with 99% query coverage and 100% identity with a predicted length of 314 amino acids (AA). The sequences ID was used to retrieve the PDB structure of protein, however no structure was reported. Therefore, SWISSMODEL was used to model the structure of RepA gene. Four structures from the PDB were identified as possible templates: the percent identities for 4PQK (58%), 4PTA (56%), 4PQL (48%), and 4PT7 (48%). Eventually, structure 4PQK was chosen as a template because of its strong resemblance to the target structure as shown in Figure 7.

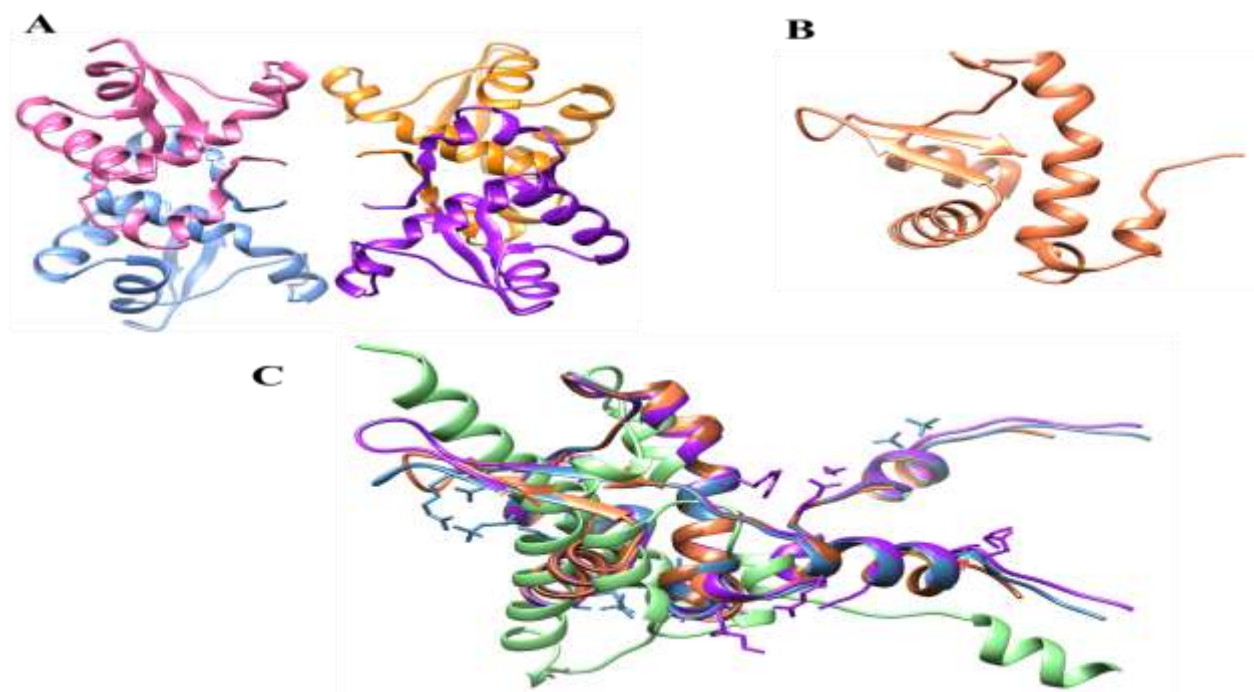


Figure 7: The 3D structure of RepA modeled via SWISSMODEL (A) tetramer (B) Monomer (chain A), and (C) model protein (coral) superimposed on the templates 4PQK (green), 4PTA (sienna), 4PQL (purple), and 4PT7 (steel blue).

Moreover, the modeled structure was validated via different tools merged in SWISSMODEL i.e., Ramachandran Plot, ProSa Web and quality assessment. It shows that the modeled structure is 96% validated having residues in allowed region. The z-score less than 1 and quality of RepA protein structure was also validated the model generated via SWISSMODEL (Figure 8).

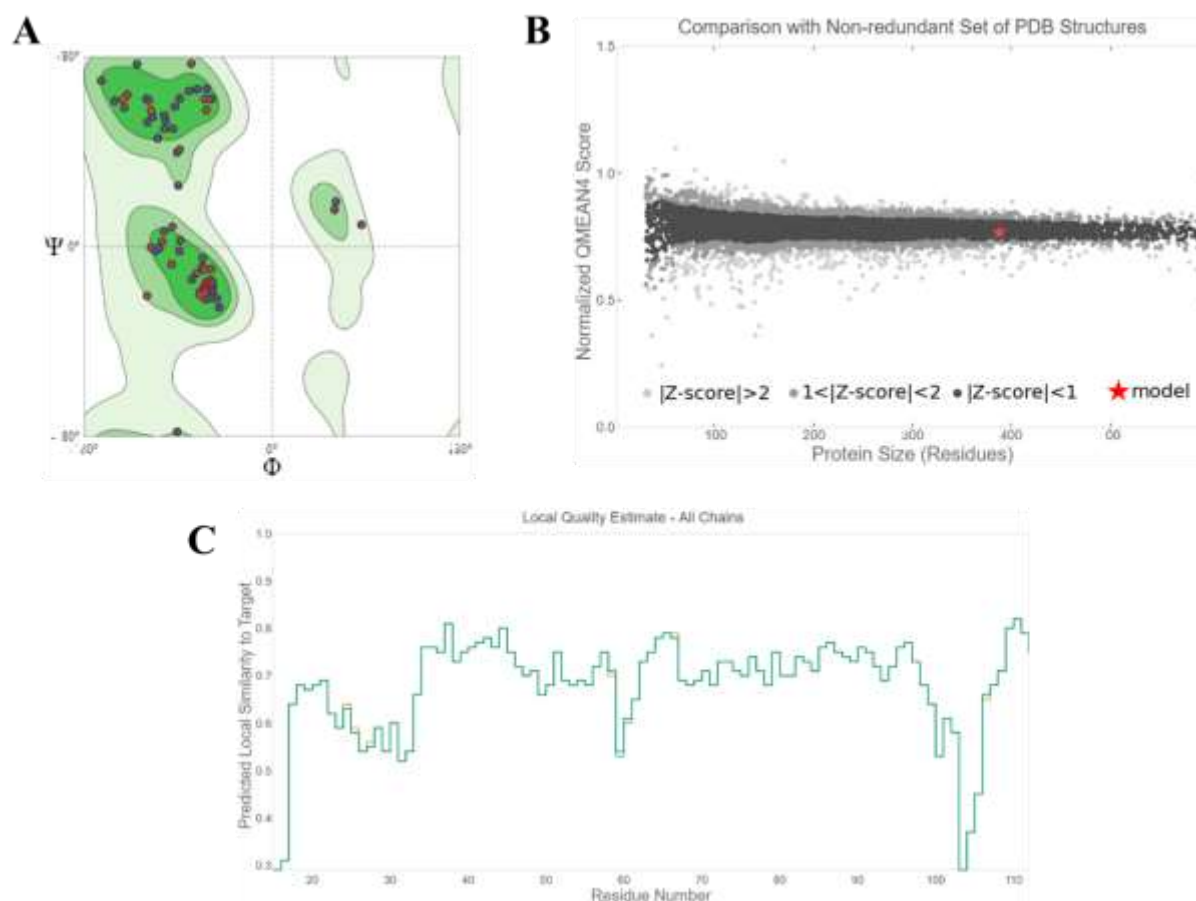


Figure 8: Validation of RepA modeled structure through SWISSMODEL. (A) Ramachandran Plot showing the 96% residues of protein within the allowed region, (B) z-score generated showing the validity for modeled structure i.e., <1 , and (C) quality prediction of protein structure.

3.10.2. Virtual Screening and Molecular Docking Studies

Molecular docking has potential to predict a ligand's primary protein-binding mechanism at the subatomic level (s). The results of AutoDock showed that the ligand might be bound in a number of different conformations and orientations inside the active site of the protein. Optimal ligand in molecular docking is the one that binds as shallowly as possible with its target protein and receptor protein. Multiple conformations were found, each with a different binding energy. Low binding-energy conformations are favored because they lead to lower energy complexes, which in turn indicates that ligand-active site interactions occur spontaneously (i.e., more stable). The binding energy of these compounds i.e., C1, C2, C3 and C4 were predicted as -5.11, -6.94, -7.34, and -5.48 kcal/mol, respectively. Therefore, the following order based on the docking scores was observed: C3 > C2 > C4 > C1

3.10.3. Interaction Analysis of Shortlisted Compounds

The compound (C1) was observed to mediate five hydrogen bonds as hydrogen acceptors from the Lys85, Lys88, and Glu89 inside the binding pocket of RepA protein with a bond length of 2.8-3.2Å. However, compound (C2) was observed to mediate two hydrogen bonds as hydrogen donor to Arg16, and Tyr 18, and four hydrogen bonds as hydrogen acceptor

from Gln19, and Leu20 having a bond distance of 2.7-32Å and binding energy as -0.5 to -5 kcal/mol. Whereas, compound (C3) mediates seven hydrogen bonds one as donor and seven as hydrogen acceptor from Tyr18, Arg16, Gln19, leu20, and Phe17 (bond lengths ranging from 2.6 nm to 3.94 nm), resulting in the top most best fit compound with in the binding pocket of RepA showing highest binding affinity of -7.3 kcal/mol. While compound (C4) was observed to form six hydrogen bonds, two as hydrogen donor and four as hydrogen acceptor through Tyr18, Arg16, Gln19, and Leu20, respectively (Figure 9).

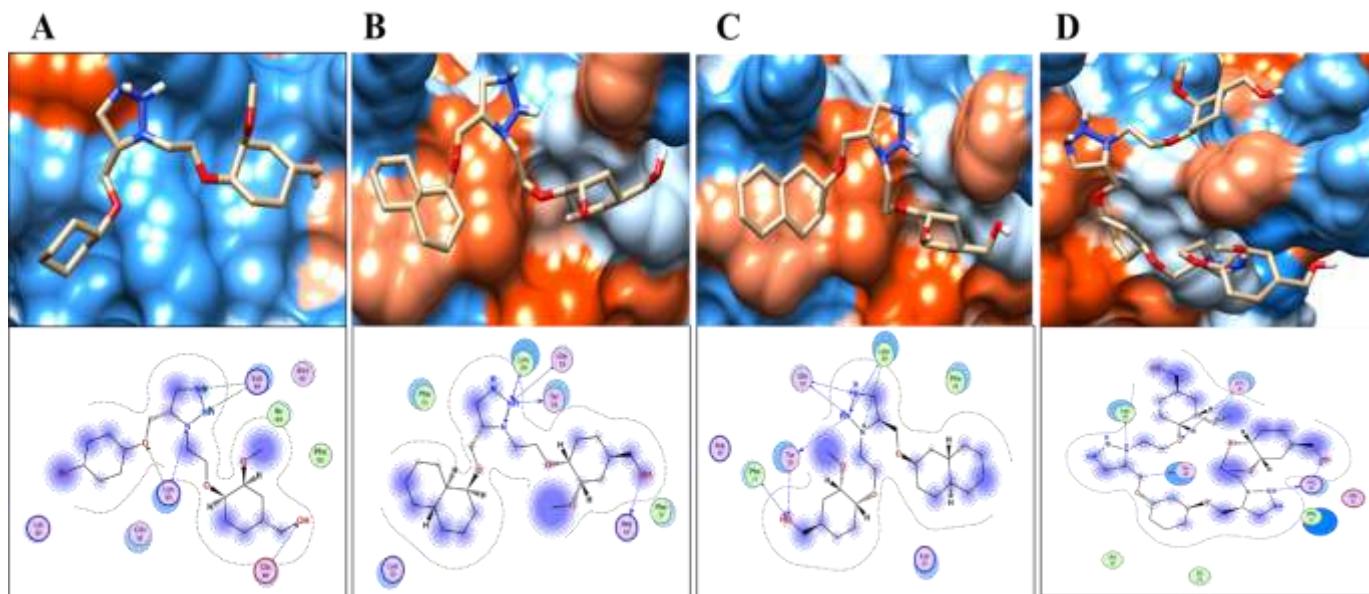


Figure 9: Docking studies of (A) C1, (B) C2, (C) C3, and (D) C4 generated through MOE tool.

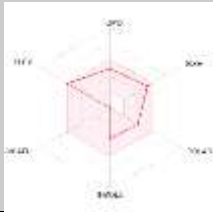
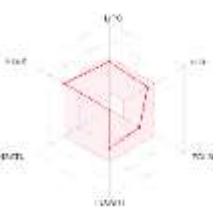
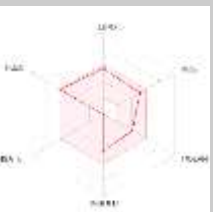
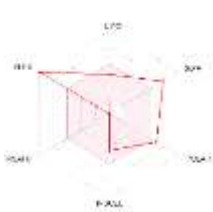
The total binding affinity of these compounds for RepA is shown in Table 6 by the prominence of interactions induced by Lys 88, Lys 85, Tyr18, Arg16, Leu 20, and Gln 19.

Table 5: The interaction detail of shortlisted compounds**3.10.4. ADMET-TOX Profiling**

S. No.	Compounds	Ligand	Receptor	Interaction	Distance	E (kcal/mol)	Binding score (kcal/mol)	Predicted Ki (μm)
1	C1	O7	CB LYS 85	H-acceptor	2.83	-0.5	-5.11	180.84
		N12	NZ LYS 88	H-acceptor	3.03	-3.7		
		N13	NZ LYS 88	H-acceptor	2.83	-6.0		
		N14	CA LYS 85	H-acceptor	3.28	-0.7		
		O27	CA GLU 89	H-acceptor	2.82	-0.7		
2	C2	N12	O TYR 18	H-donor	2.93	-0.9	-6.94	8.23
		O26	O ARG 16	H-donor	2.71	-2.1		
		N12	CA GLN 19	H-acceptor	3.06	-1.5		
		N12	N LEU 20	H-acceptor	2.75	-5.0		
		N13	N LEU 20	H-acceptor	3.08	-0.7		
		N13	CB LEU 20	H-acceptor	3.29	-0.8		
3	C3	N16	O TYR 18	H-donor	2.63	-0.8	-7.34	4.15
		N15	CA GLN 19	H-acceptor	3.32	-0.9		
		N16	CA GLN 19	H-acceptor	3.02	-1.6		
		N16	N LEU 20	H-acceptor	2.79	-5.1		
		N17	CB LEU 20	H-acceptor	3.49	-0.7		
		O30	CA PHE 17	H-acceptor	3.41	-0.7		
		O30	N TYR 18	H-acceptor	3.03	-2.5		
4	C4	C28	O TYR 18	H-donor	2.90	-0.5	-5.48	96.18
		N12	O ARG 16	H-donor	2.55	-1.1		
		N33	N LEU 20	H-acceptor	3.08	-4.4		
		O36	CA GLN 19	H-acceptor	3.67	-0.5		
		O43	NE2 GLN 19	H-acceptor	3.22	-1.0		
		O26	N ARG 16	H-acceptor	3.44	-0.7		

Confirming the efficacy and safety of the drugs requires an understanding of their pharmacokinetic properties and toxicity profile. The use of pharmacokinetic (PK) parameters in the assessment and forecasting of biological processes such as the toxicity or therapeutic efficacy of a substance. The Swiss ADME online tool was used to determine the pharmacokinetic properties of these substances based on their BBB crossing ability, toxicological evaluations, ADME profiles, and drug-likeness. Permeability to HIA was noted for all substances. The drug similarity measure was established using the Lipinski rule of 5. While chemicals C1, C2, and C3 all abided by the Lipinski rule of 5, compound C4 was in violation of the first rule. The capacity of a chemical to enter the central nervous system is characterized by its ability to cross the Blood-Brain Barrier (BBB). Each of these four substances is impermeable to the BBB. To penetrate the brain, a value of CNS > -2 was determined (CNS). The CNS permeability of these shortlisted compounds was -3.131, -2.742, -2.742, and -3.536, indicating that they are CNS non-accessible (Table 5).

Table 6: ADME properties analysis of shortlisted compounds

Name	Water Solubility	CaCo2 permeability	HIA	Skin Permeability	BBB permeability	Lipinski Violation	Bioavailability radar
C1	-4.537	0.994	94.40 3	-2.736	No	Yes	
C2	-4.823	0.931	94.02 3	-3.228	Yes	Yes	
C3	-4.849	0.902	93.99 6	-3.226	Yes	Yes	
C4	-4.329	0.153	78.91 2	-2.664	No	No	

All four chemicals were predicted to be safe and non-carcinogenic based on results from the AMES (assay to assess reverse mutation in Salmonella) and the carcinogenic profile evaluation. The four lead-like compounds were tested for safety according to the Lipinski rule of five, which also took into account their pharmacokinetic and toxicological properties (Table 7). However, C1 and C4 were shown to be hepatotoxic.

Table 7: Toxicity analysis of shortlisted four compounds

Name	Max. tolerated dose (human)	Minnow toxicity	<i>T. Pyriformis</i> toxicity	Oral Rat Acute Toxicity (LD50)	Ames Test	Hepatotoxic	Skin Sensitization
C1	-0.271	1.566	0.591	2.943	Yes	Yes	No
C2	-0.84	0.241	0.557	3.255	No	No	No
C3	-0.853	0.199	0.561	3.244	No	No	No
C4	-0.497	2.031	0.285	3.168	No	Yes	No

4. CONCLUSION

Nosocomial infections are becoming more common, and the strains of MRSA being identified from them are showing greater resistance to multiple antimicrobials. In clinical laboratory settings, a fast, traditional identification approach based on phenotypic and genotypic features is appropriate. This study delineated the origin of resistance in *S. aureus* by identifying not only its known resistant genes i.e., *mecA* and *vanA*, but also the Plasmid mediated resistance gene, *RepA* gene, which is located on plasmid, but the mechanism of action of the gene is still unknown. In addition, methods like *in silico* screening may provide early drug development research with quick and precise information on novel medicinal substances. As a result, the pharmacological effects of four synthetic compounds (C1, C2, C3, and C4) against *RepA* were hypothesized in the study. The -7.34 kcal/mol chemical C3 was chosen as a promising inhibitor in virtual screening, molecular docking, and antimicrobial activity. Future, *in vivo* studies can confirm these compounds, especially C3, as effective antibacterials in combating infections caused by *S. aureus*.

Declarations:**Ethics approval and consent to participate**

Not Applicable

Consent for publication

Not Applicable

Availability of data and materials

All data generated or analyzed during this study are included in this published article.

Competing interests

The authors declare that they have no competing interests.

Funding

No Funding was available for the project.

Authors' contributions

Kiran Fatima: Investigation: Conducting a research and investigation process, specifically performing the experiments, or data/evidence collection; preparing draft; **Kashif Ali:** Supervision: oversight and leadership responsibility for the research activity planning and execution, including mentorship external to the core team; **Khwaja Ali Hasan:** Molecular Investigation; **Neha Farid:** Manuscript writing, formal analysis and final composing of the manuscript; **Mumtaz Hussain:** Synthesized Triazole's compound and manuscript editing; **Kanwal Khan, Khurshid Jalal and Reaz Uddin:** *In silico* and biocomputational studies; **Zahid Hussain:** Manuscript editing.

References

1. Becker K, *et al.* (2018) Plasmid-encoded transferable *mecB*-mediated methicillin resistance in *Staphylococcus aureus*. *Emerging infectious diseases* **24**(2): 242.
2. Friedman ND, *et al.* (2016) The negative impact of antibiotic resistance. *Clinical Microbiology Infection*. **22**(5): 416-422.

3. Jalal K, *et al.* (2021) Identification of a Novel Therapeutic Target against XDR *Salmonella Typhi* H58 Using Genomics Driven Approach Followed Up by Natural Products Virtual Screening. *Microorganisms* **9**(12): 2512.
4. Enrigh MC, *et al.* (2002) The evolutionary history of methicillin-resistant *Staphylococcus aureus* (MRSA). *Proceedings of the National Academy of Sciences* **99**(11): 7687-7692.
5. Deschaght P, *et al.* (2009) Comparison of the sensitivity of culture, PCR and quantitative real-time PCR for the detection of *Pseudomonas aeruginosa* in sputum of cystic fibrosis patients. *BMC microbiology* **9**(1): 1-7.
6. Kallen AJ, *et al.* (2010) Health care-associated invasive MRSA infections, 2005-2008. *Jama* **304**(6): 641-647.
7. Omrani-Navai V, *et al.* (2017) Human papillomavirus and gastrointestinal cancer in Iranian population: A systematic review and meta-analysis. *Caspian Journal of Internal Medicine* **8**(2): 67.
8. Schumacher MA, *et al.* (2014) Mechanism of staphylococcal multiresistance plasmid replication origin assembly by the RepA protein. *Proceedings of the National Academy of Sciences* **111**(25): 9121-9126.
9. Biswas S, *et al.* (2015) "Multidrug resistant pathogenic *Staphylococcus aureus* in the pimples. *Medical Science* **16**: 41-50.
10. Rashdan HR and Shehadi IA (2022) Triazoles synthesis & applications as nonsteroidal aromatase inhibitors for hormone-dependent breast cancer treatment. *Heteroatom Chemistry* **2022**.
11. Zhang L, *et al.* (2005) Ruthenium-catalyzed cycloaddition of alkynes and organic azides. *Journal of the American Chemical Society* **127**(46): 15998-15999.
12. Rodgers JD, *et al.* (1999) Comparison of *Staphylococcus aureus* recovered from personnel in a poultry hatchery and in broiler parent farms with those isolated from skeletal disease in broilers. *Veterinary microbiology* **69**(3): 189-198.
13. Morris GM, *et al.* (2001) AutoDock. Automated docking of flexible ligands to receptor-User Guide.
14. Zoetendal EG, *et al.* (2006) Isolation of DNA from bacterial samples of the human gastrointestinal tract. *Nature protocols* **1**(2): 870-873.
15. Thwala T, *et al.* (2022) Antimicrobial Resistance, Enterotoxin and mec Gene Profiles of *Staphylococcus aureus* Associated with Beef-Based Protein Sources from KwaZulu-Natal Province, South Africa. *Microorganisms* **10**(6): 1211.
16. Tamura K, *et al.* (2011) MEGA5: molecular evolutionary genetics analysis using maximum likelihood, evolutionary distance, and maximum parsimony methods. *Molecular biology evolution* **28**(10): 2731-2739.
17. Sofy, AR, *et al.* (2020) Polyvalent phage CoNSHP-3 as a natural antimicrobial agent showing lytic and antibiofilm activities against antibiotic-resistant coagulase-negative *Staphylococci* strains. *Foods* **9**(5): 673.
18. Treves DS (2010) Review of three DNA analysis applications for use in the microbiology or genetics classroom. *Journal of microbiology biology education* **11**(2): 186-187.
19. Freeman D, *et al.* (1989) New method for detecting slime production by coagulase negative *Staphylococci*. *Journal of clinical pathology* **42**(8): 872-874.
20. Patel JB, *et al.* (2015) Performance standards for antimicrobial susceptibility testing: twenty-fifth informational supplement.
21. Georgieva RN, *et al.* (2008) Identification and *in vitro* characterisation of *Lactobacillus plantarum* strains from artisanal Bulgarian white brined cheeses. *Journal of Basic Microbiology* **48**(4): 234-244.
22. Liu X, *et al.* (2012) Curing of plasmid pXO1 from *Bacillus anthracis* using plasmid incompatibility. *PloS one* **7**(1): e29875.
23. Leshem T, *et al.* (2022) Incidence of biofilm formation among MRSA and MSSA clinical isolates from hospitalized patients in Israel. *Journal of Applied Microbiology* **133**(2): 922-929.
24. Kiefer F, *et al.* (2009) The SWISS-MODEL Repository and associated resources. *Nucleic acids research* **37**(suppl_1): D387-D392.

25. Huey R, *et al.* (2012) Using AutoDock 4 and AutoDock vina with AutoDockTools: a tutorial. The Scripps Research Institute Molecular Graphics Laboratory **10550**: 92037.
26. O'Boyle NM, *et al.* (2011) Open Babel: An open chemical toolbox. Journal of cheminformatics **3**(1): 1-14.
27. Miteva MA, *et al.* (2010) Frog2: Efficient 3D conformation ensemble generator for small compounds. Nucleic acids research **38**(suppl_2): W622-W627.
28. Turnipseed H (2022) Effect Of Disinfectants On The Formation Of Biofilms By Methicillin-Resistant *Staphylococcus aureus* (MRSA)."
29. Khan T, Alzahrani OM, Sohail M, Hasan KA, Gulzar S, Rehman AU, Mahmoud SF, Alswat AS, Abdel-Gawad SA (2022) Enzyme profiling and identification of endophytic and rhizospheric bacteria isolated from *Arthrocnemum macrostachyum*. Microorganisms **10**(11): 2112.